Daniel Gogny Jubilee
Bruyeres-le-Chatel
May 30-31, 2006

Monte Carlo Shell Model calculations on exotic nuclei

Takaharu Otsuka University of Tokyo / RIKEN

Diagonalization of Hamiltonian matrix

$$\begin{pmatrix} * & * & * & * & * & \cdot & \cdot \\ * & * & * & * & \cdot & \cdot & \cdot \\ * & * & * & \cdot & \cdot & \cdot & \\ * & * & \cdot & \cdot & \cdot & \cdot & \\ \cdot & \cdot & \cdot & \cdot & & & \\ \cdot & & & & & & \end{pmatrix} \xrightarrow{\text{diagonalization}} \begin{pmatrix} \varepsilon_1 & & & & & 0 \\ & \varepsilon_2 & & & & \\ & & \varepsilon_3 & & & \\ & & & \cdot & & \\ & & & & \cdot & \\ 0 & & & & & \cdot \end{pmatrix}$$

Conventional Shell Model calculation
All Slater determinants

$$\begin{pmatrix} * & * & * & \cdot \\ * & * & * & \cdot \\ * & * & \cdot & \\ \cdot & \cdot & & \end{pmatrix} \xrightarrow{\text{diagonalization}} \begin{pmatrix} \varepsilon_1' & & & 0 \\ & \varepsilon_2' & & \\ & & \cdot & \\ 0 & & & \cdot \end{pmatrix}$$

Quantum Monte Carlo Diagonalization method
Important bases are selected

(about 30 dimension)

Progress in shell-model calculations and computers

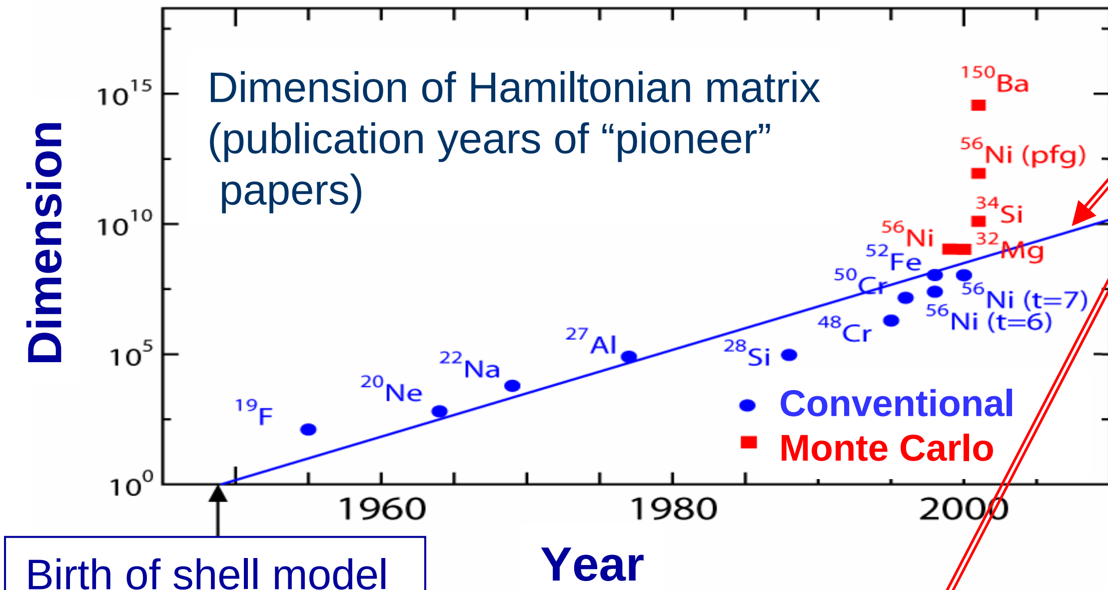

Lines : 10^5 / 30 years

More cpu time for heavier or more exotic nuclei

^{238}U one eigenstate/day in good accuracy requires 1PFlops

Birth of shell model (Mayer and Jensen)

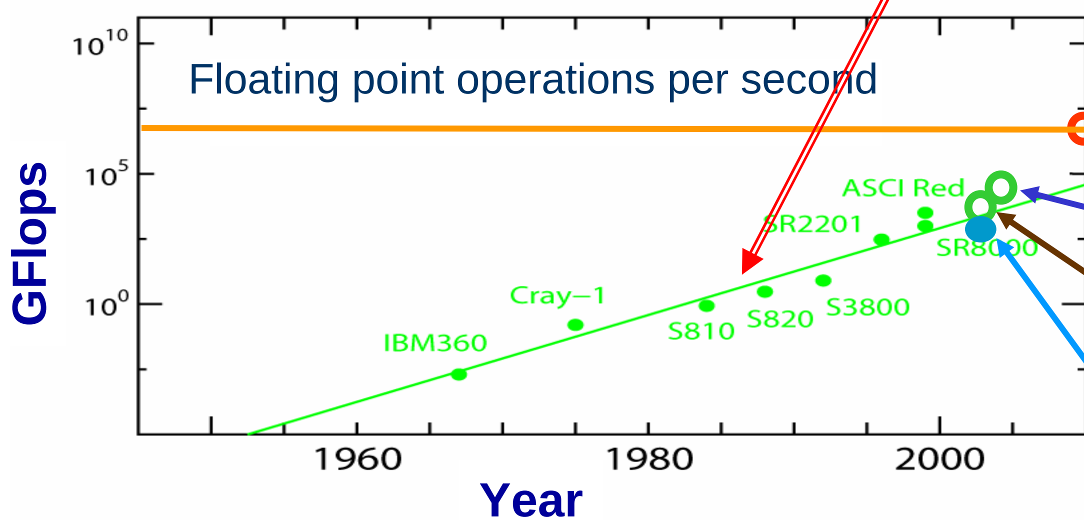

京速計算機 (Japanese challenge)

Blue Gene

Earth Simulator

Our parallel computer

Basic points of Monte Carlo Shell Model (I)

Two-body interaction can be rewritten as $V = (1/2)\, \Sigma_\alpha\ \mathbf{v}_\alpha\, \mathbf{O}_\alpha{}^2$

α : index
$\mathbf{O}_\alpha$: one-body operators (rearranged by diagonalization)

Hubberd-Stratonovichi transformation

True eigenstate : $\psi = \Sigma_\sigma\, e^{-\beta h(\sigma)}\ e^{-\beta h(\sigma')}\ \ldots\ \psi_0$

imaginary time (β) evolution by one-body field $h(\sigma)$

One-body operator is introduced as $h(\sigma) = \Sigma_\alpha\ \mathbf{s}_\alpha\, \sigma_\alpha\, \mathbf{v}_\alpha\, \mathbf{O}_\alpha$

σ_α : random number σ : set of σ_α's
s_α : phase

Basic points of Monte Carlo Shell Model (II)

True eigenstate : $\psi = \Sigma_{\sigma,\sigma',\,\ldots}\, e^{-h(\sigma)}\, e^{-h(\sigma')}\, \ldots\, \psi_0$

Use $\phi\,(\sigma,\sigma',\ldots) = e^{-\beta h(\sigma)}\, e^{-\beta h(\sigma')}\, \ldots\, \psi_0$
as a basis for shell-model diagonalization

$\phi\,(\sigma,\sigma',\ldots)$ are selected and refined :

(i) Random sampling -> only those lowering energy are kept
(ii) Polished by varying **$\sigma,\sigma',\ldots$** gradually (random noise reduced)
(iii) Symmetry restoration (Angular momentum, parity)

Slater determinants or Cooper-pair type wave functions are used

Usually, 20~50 bases are kept (many more thrown away)

Magnetic moment of 2^+ level of Xe isotopes

* G. Jakob et al. Phys. Rev. C65, 024316 (2002)

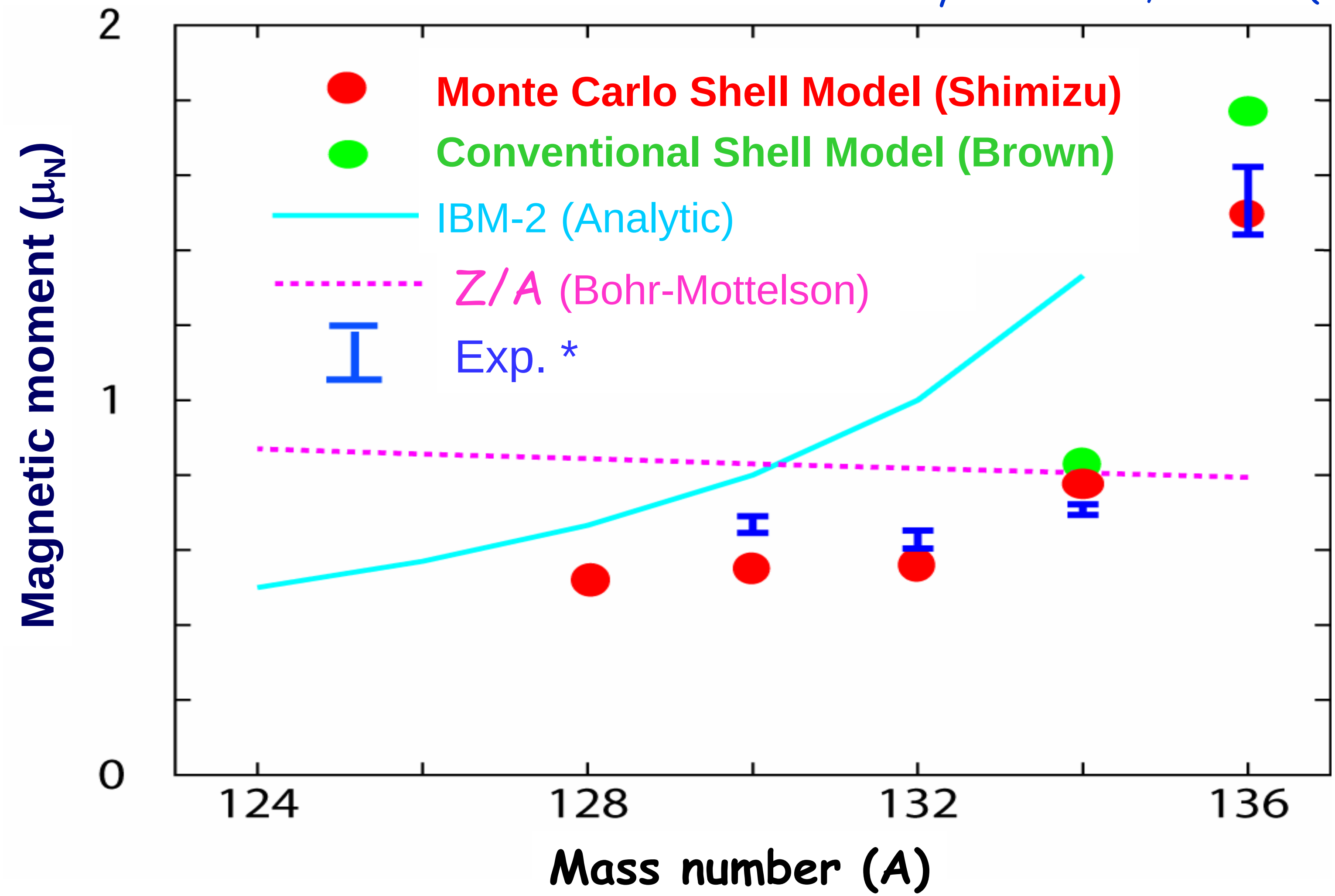

More difficult in computation

A=128 : 10^{13} dimension

In the study of structure of

neutron-rich exotic unstable nuclei,

Some “surprises” in recent experiments on nuclei with N ~ 18, 19 :

Extremely low-lying intruder states in

^{31}Mg (Z=12, N=19)

^{29}Na (Z=11, N=18)

^{30}Na (Z=11, N=19)

These have been classified as “normal nuclei” , for instance, in the Island of Inversion picture of Warburton et al.

Phys. Rev. C 41, 1147 (1990), Warburton, Brown and Becker

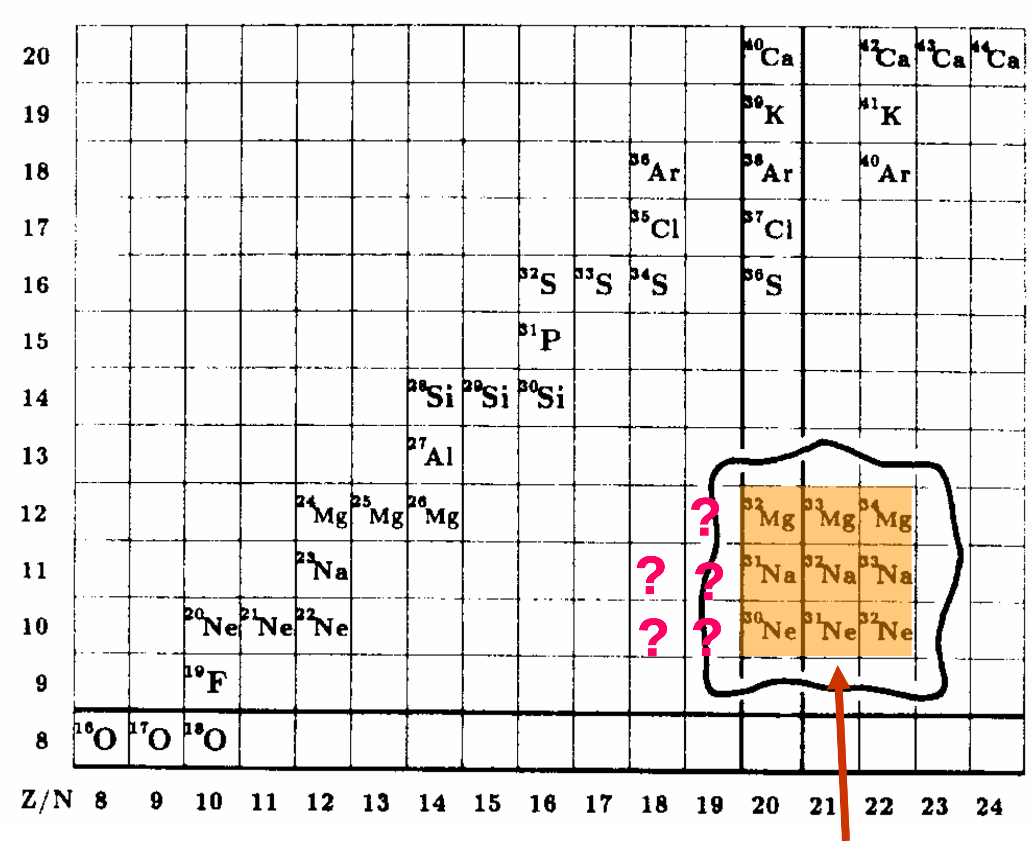

Island of Inversion :
region of intruder ground states

A sharp transition between normal and intruder

Physics Issues

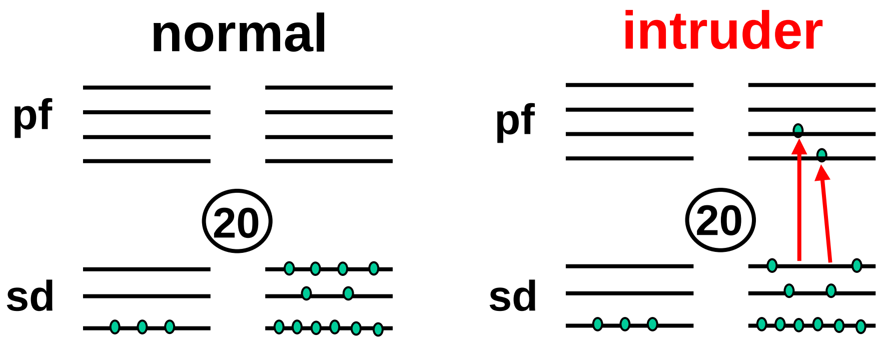

SPE Gap vs. Correlation Energy
(from a viewpoint of spherical shell)

Fully mixed calculations, e.g., Monte Carlo Shell Model, are essential

Otherwise, the gap cannot be investigated precisely

Effective single-particle energies in the "SDPF-M" interaction

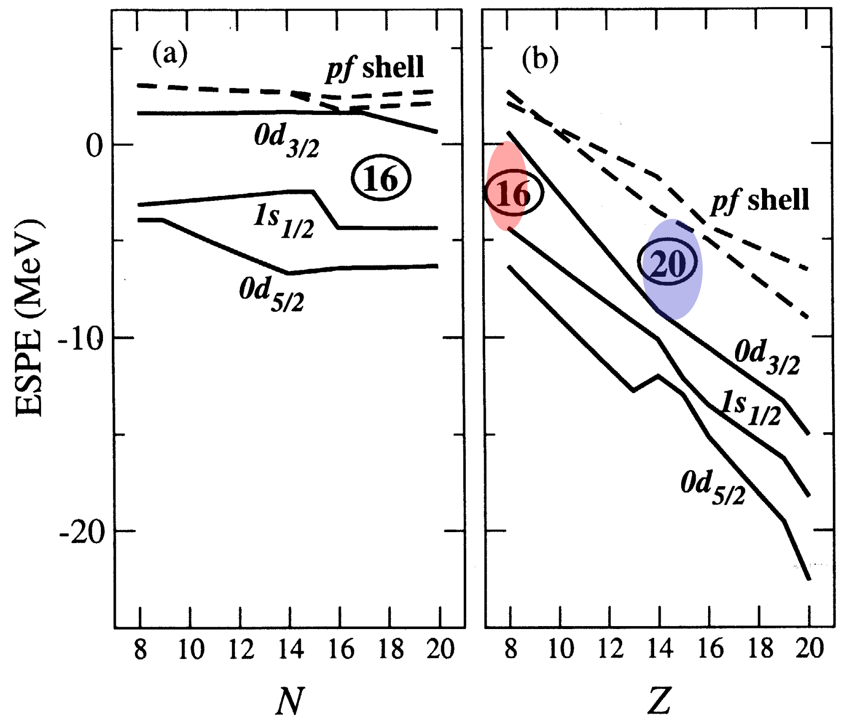

Y. Utsuno, T. Otsuka, T. Mizusaki, and M. Honma, Phys. Rev. C **60**, 054315 (1999).
T. Otsuka, M. Honma, T. Mizusaki, N. Shimizu, and Y. Utsuno, Prog. Part. Nucl. Phys. **47**, 319 (2001).

Sensitivity of intruder levels differs between semi-magic and open-shell nuclei

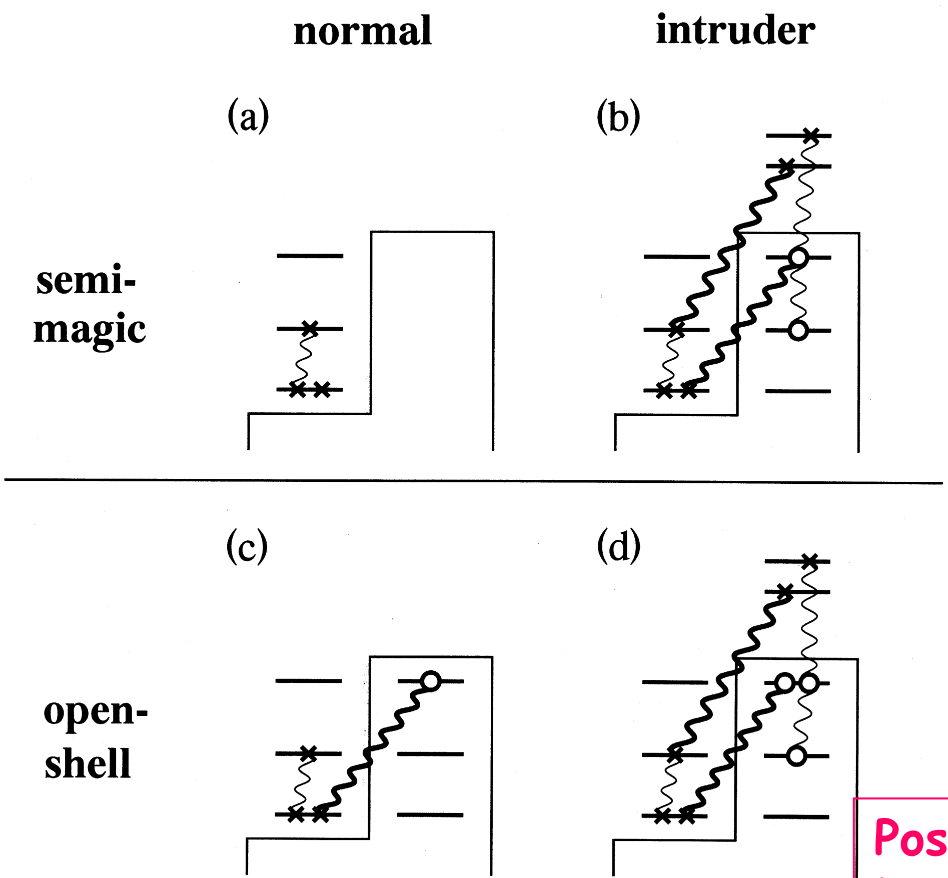

The difference in correlation energy is smaller.

Gap larger,
Correlation coupling constant larger

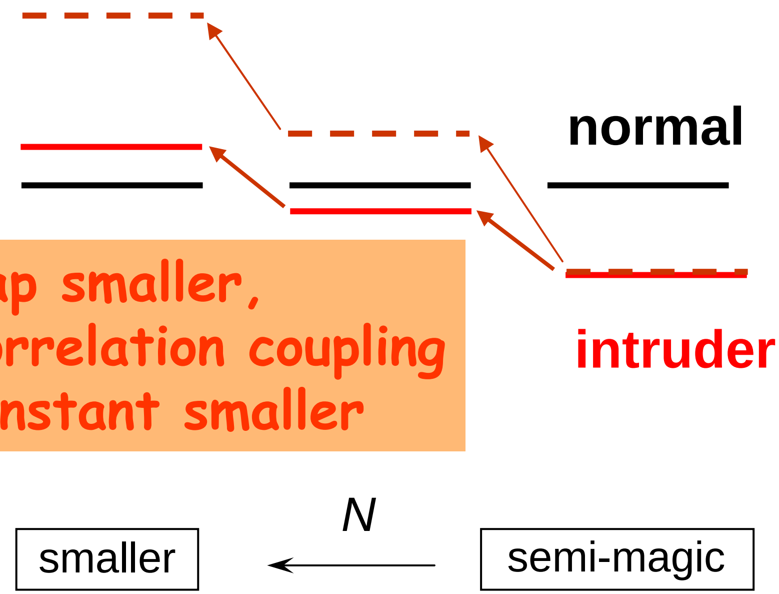

Gap smaller,
Correlation coupling constant smaller

Position of intruders is more sensitive to the gap size

Intruders are likely lower

Two Gogny(-type) interactions : D1S and GT2

Talk by Abe

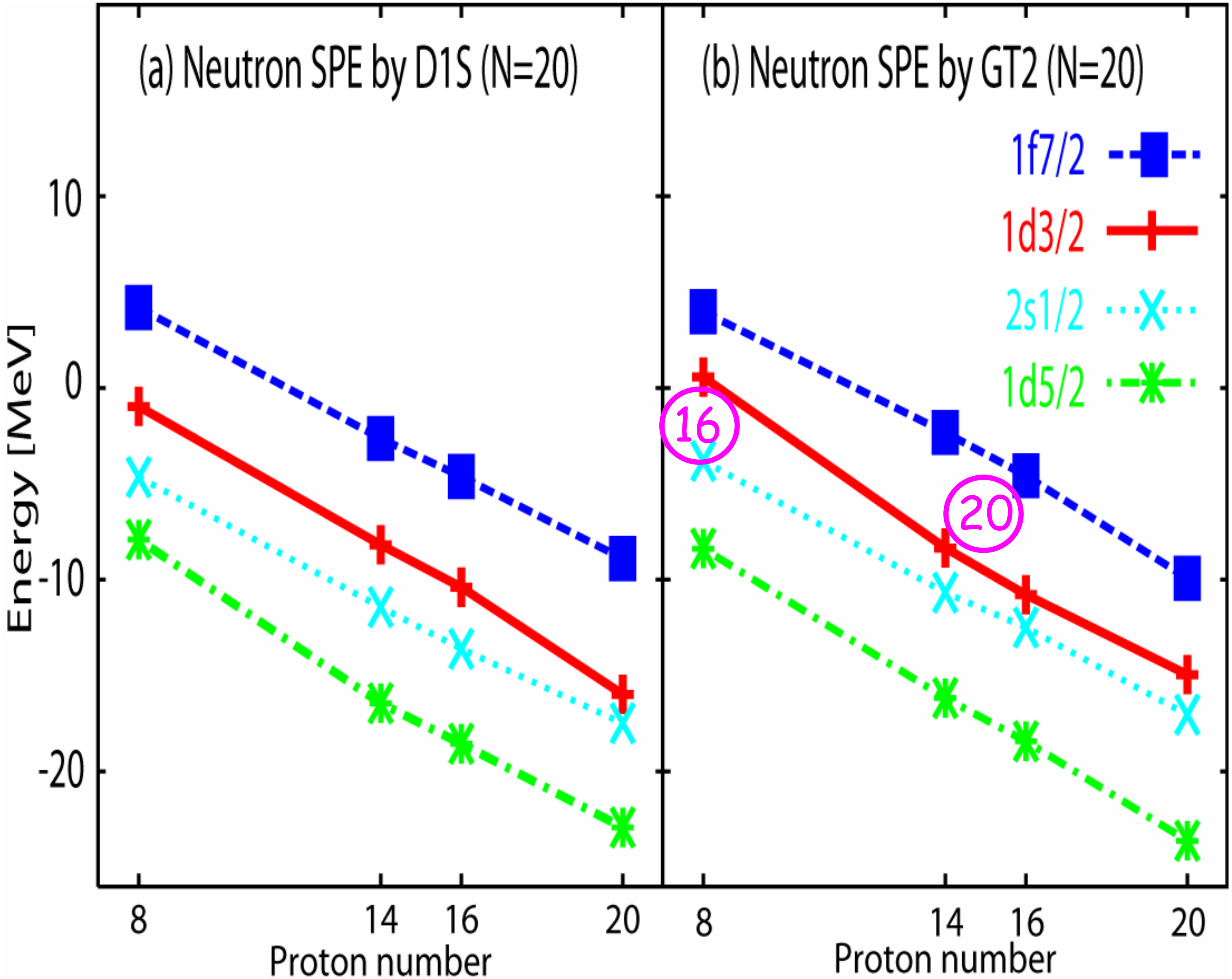

Level scheme of Na isotopes by SDPF-M interaction compared to experiment

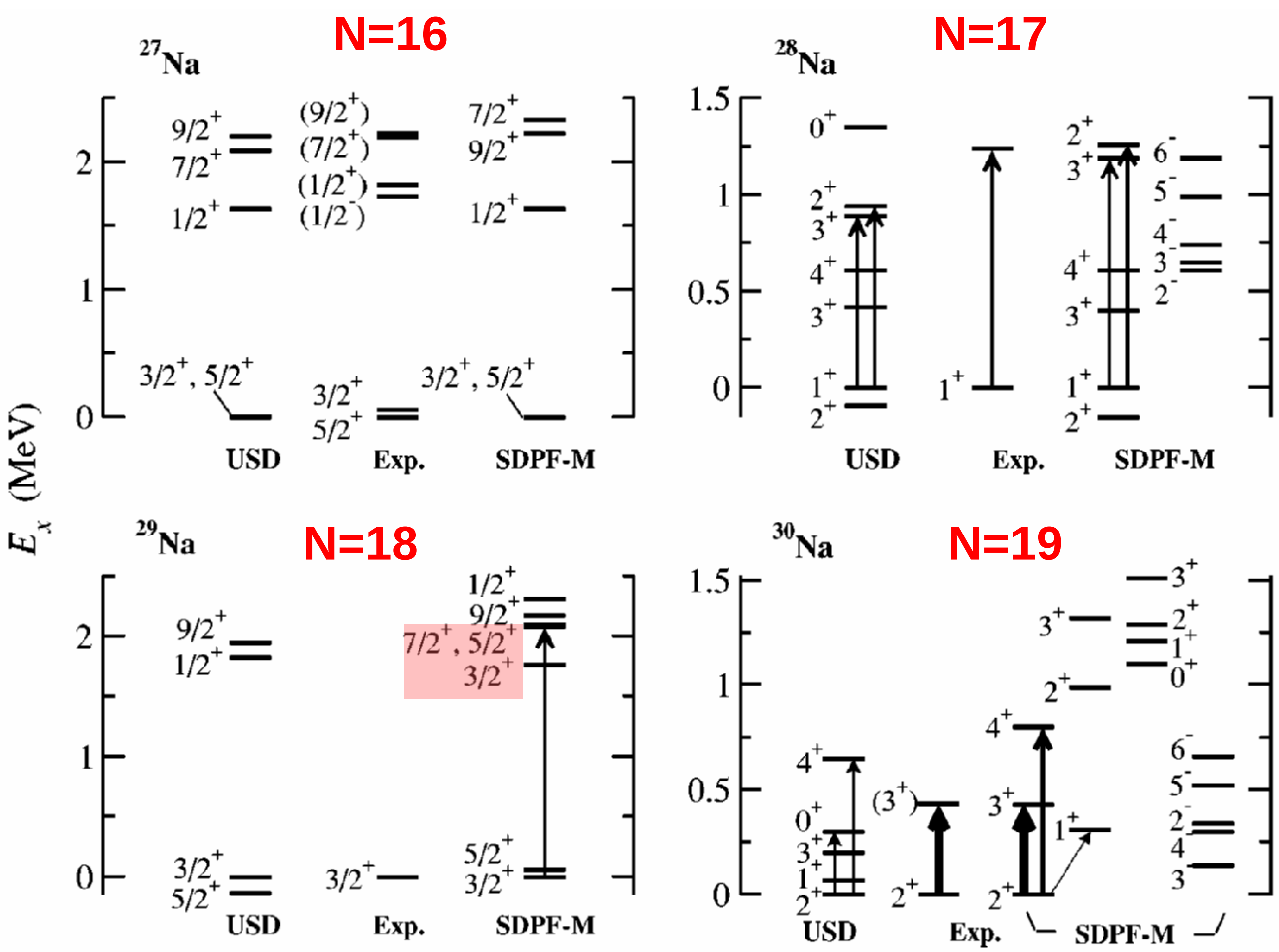

FIG. 4. Comparison of the energy levels of $^{27-30}$Na relative to the experimental ground state among the experiment (Exp.) and the shell-model calculations by the SDPF-M and the USD interactions. The $E2$ strength from the ground state is illustrated by the width of the arrow. The experimental $B(E2)$ values of ^{28,30}Na and the energy levels of ^{27}Na are taken from Refs. [25] and [36], respectively. For ^{30}Na, the levels calculated from SDPF-M interaction are grouped into four columns; the first (second) one is $K=2(1)$ rotational band dominated by intruder configurations, the third one represents spherical states which are basically of normal configurations, and negative-parity states are shown in the fourth column.

Electro-magnetic moments and wave functions of Na isotopes

— normal dominant : N=16, 17

— **strongly mixed : N=18**

— **intruder dominant : N=19, 20**

Onset of intruder dominance earlier than "island of inversion" picture (at N=20)

Phys. Rev. C 70, 044307 (2004), Y. Utsuno et al.

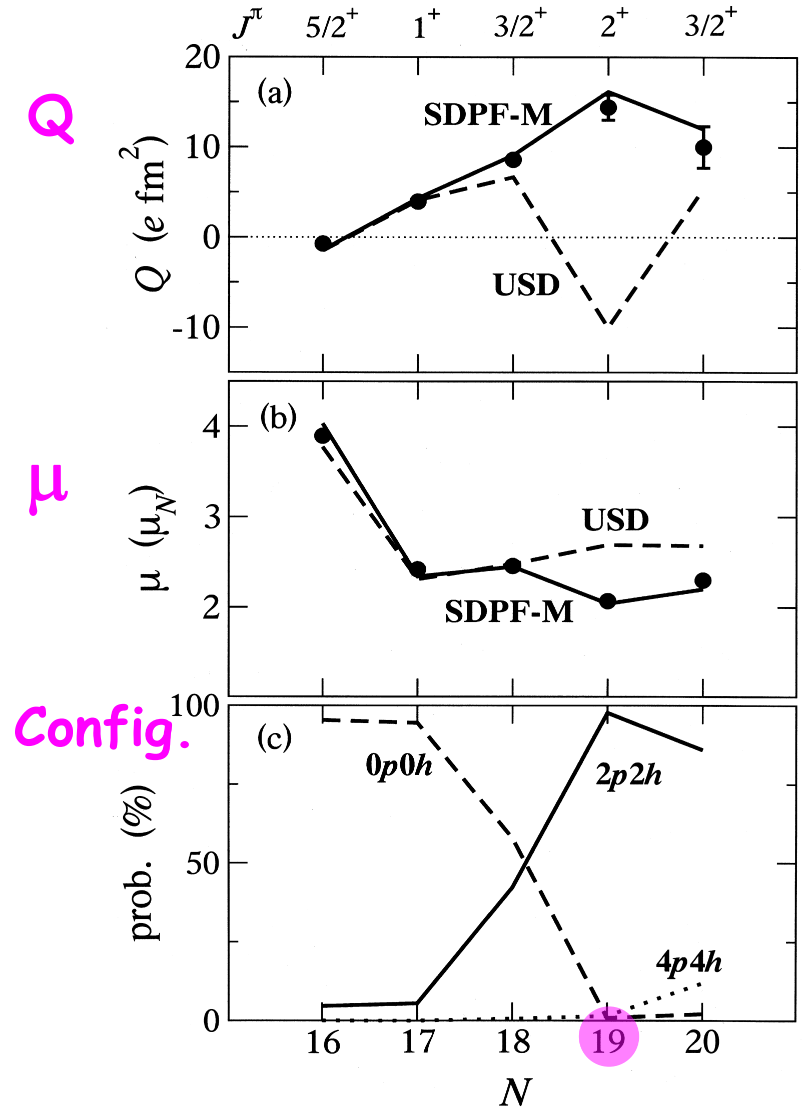

Mass systematics in Na isotopes

BROWN & WILDENTHAL

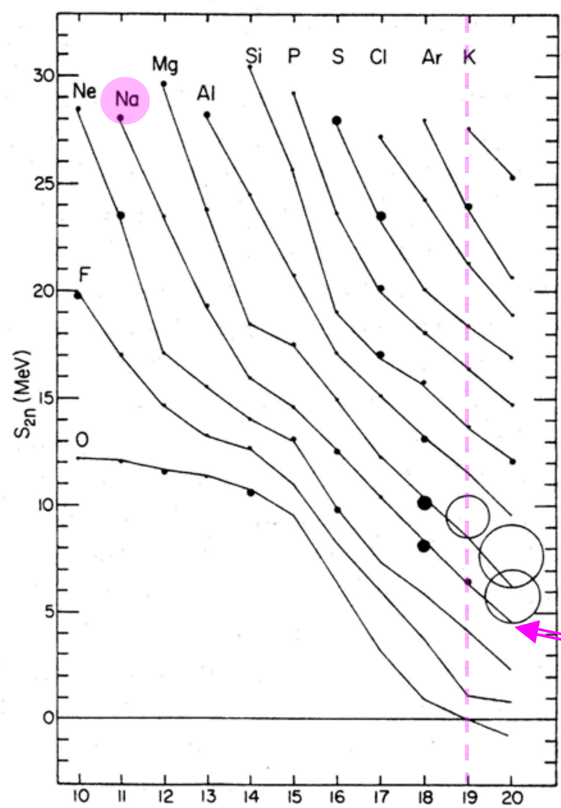

N

ure 4 Two-neutron separation energi function of the neutron n
ction 2.1

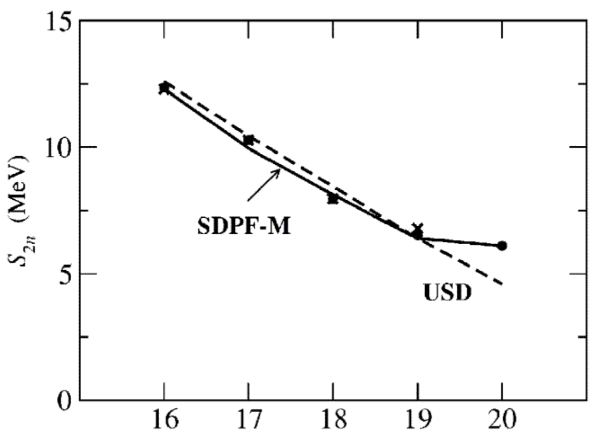

S_{2n} (MeV)

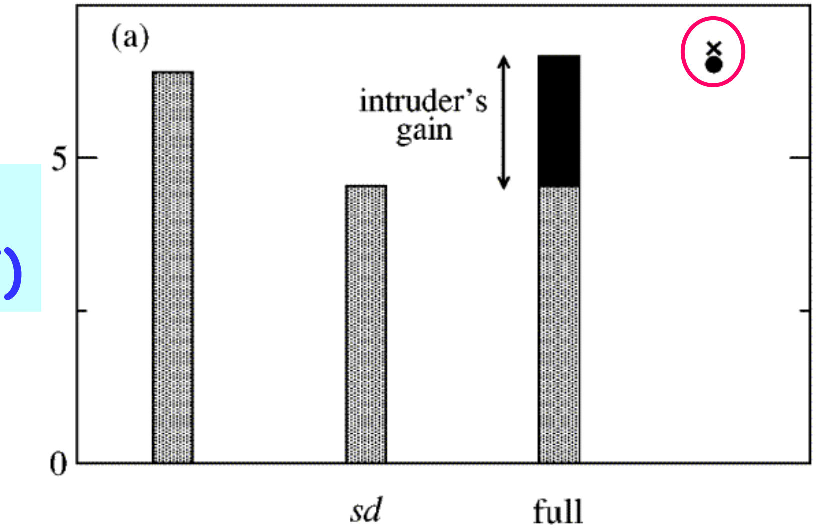

USD

SDPF-M

Exp.

Single Particle Energy (MeV)

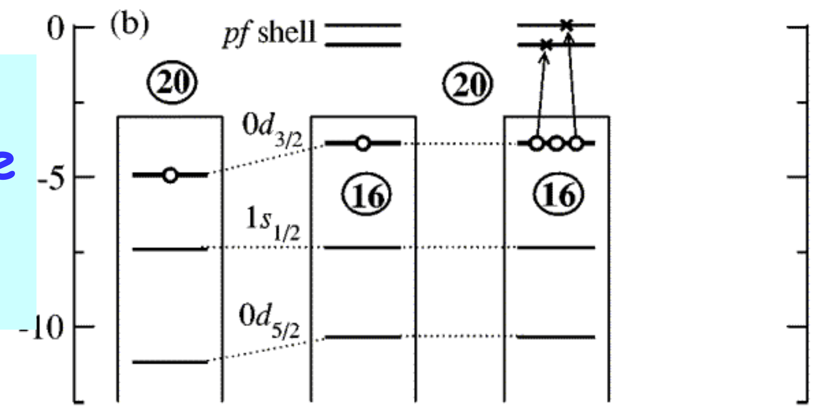

USD

SDPF-M

Phys. Rev. Lett. 94, 162501 (2005), V. Tripathi et al.

Lowest states are intruders (> 50%)

$^{29}Na_{18}$

3/2⁺, 5/2⁺ ? (from log *ft*)

zero BR

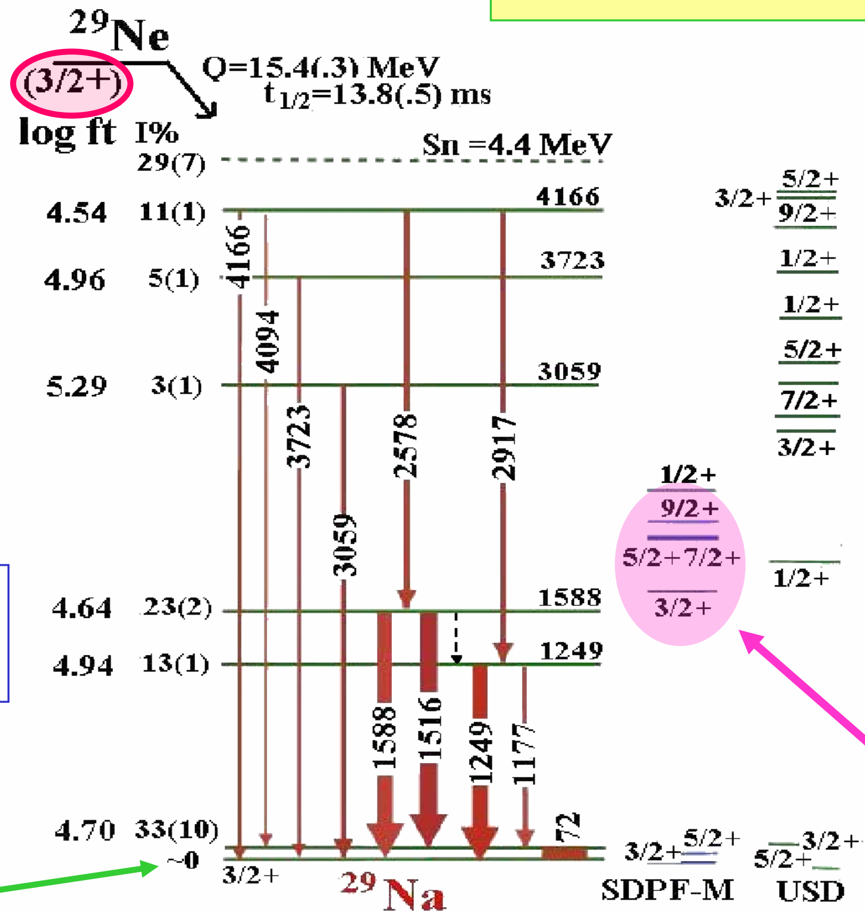

only state below 2.8 MeV by USD (large log *ft*)

4 additional states of intruder config. by SDPF-M int. (MCSM calc.)

FIG. 2 (color online). Proposed level scheme for ^{29}Na populated following the β^- decay of ^{29}Ne. The absolute β-decay branching to each level per 100 decays is indicated along with the calculated logft values. Shown on the right are shell model calculations with the USD and SDPF-M interactions.

Phys. Rev. Lett. 94, 022501 (2005), G. Neyens, et al.

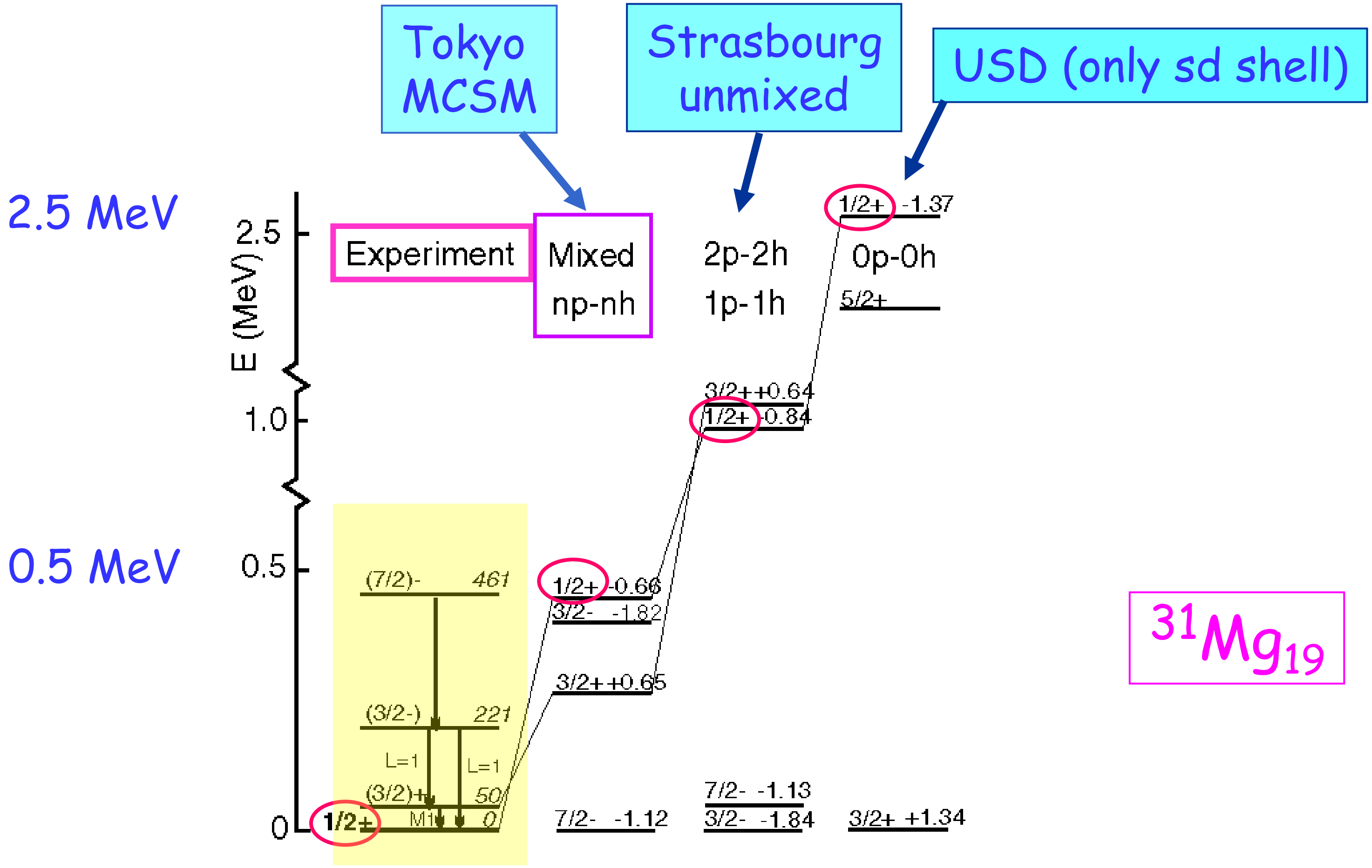

FIG. 3. Partial experimental level scheme of ^{31}Mg, with new spin/parity assignments, compared to various shell-model calculations (see text for details). The magnetic moments of theoretical levels are mentioned on the right (units μ_N).

Level scheme of ^{28}Ne

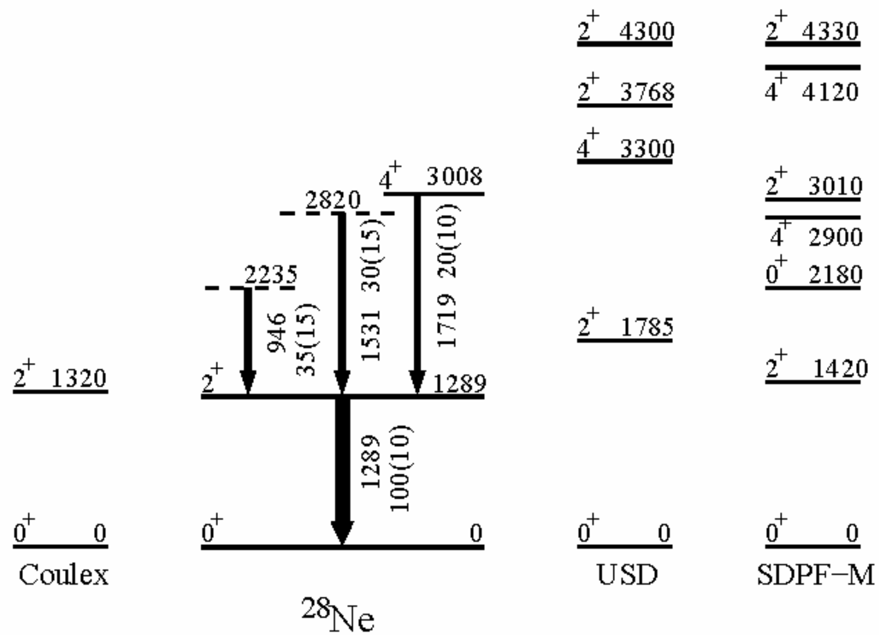

FIG. 9: Proposed level scheme of ^{28}Ne. The results of different shell model calculations [7, 22] are included in the right part of the figure. The energy of the first excited state observed in Coulomb excitation experiment is taken from Ref. [20]. The spin 4 assignment to the 3008 keV state is taken from Ref. [21].

Phys. Rev. C 41, 1147 (1990), Warburton, Brown and Becker

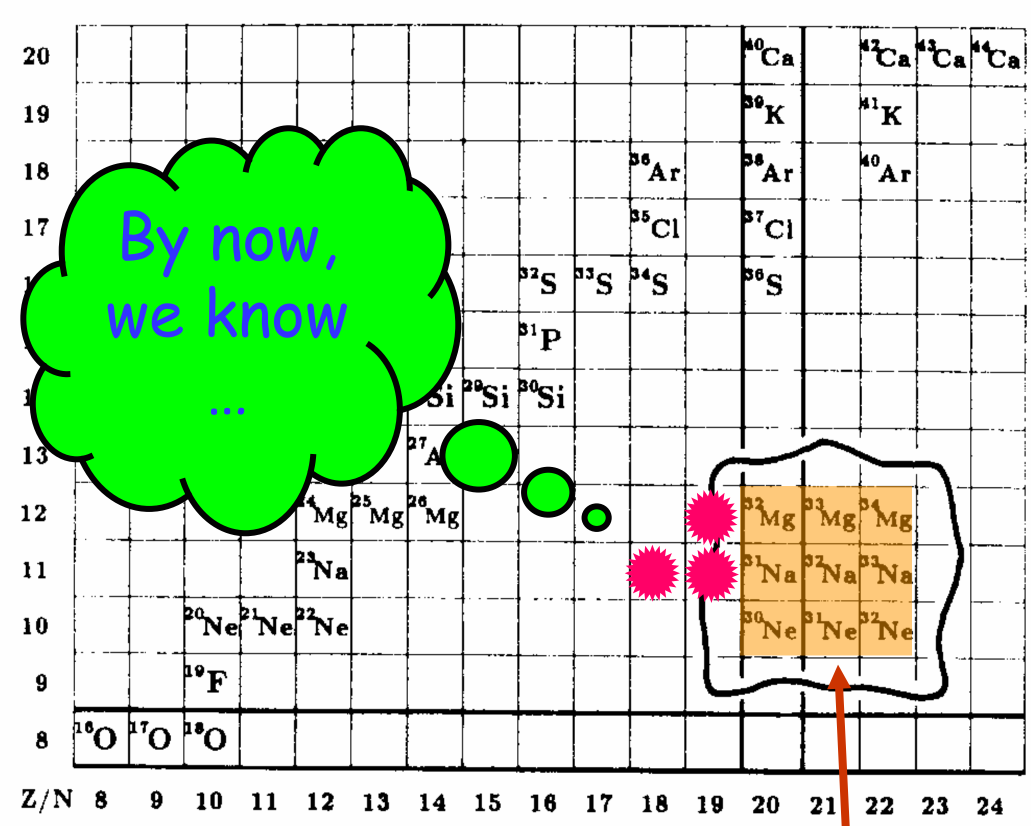

Island of Inversion :
region of intruder ground states

A sharp transition between normal and intruder

The shell model (MCSM) results have been obtained by the SDPF-M interaction for the full-*sd* + $f_{7/2}$ + $p_{3/2}$ space.

The effective gap between the sd and pf shells

Intruder low-lying states even with modest deformation

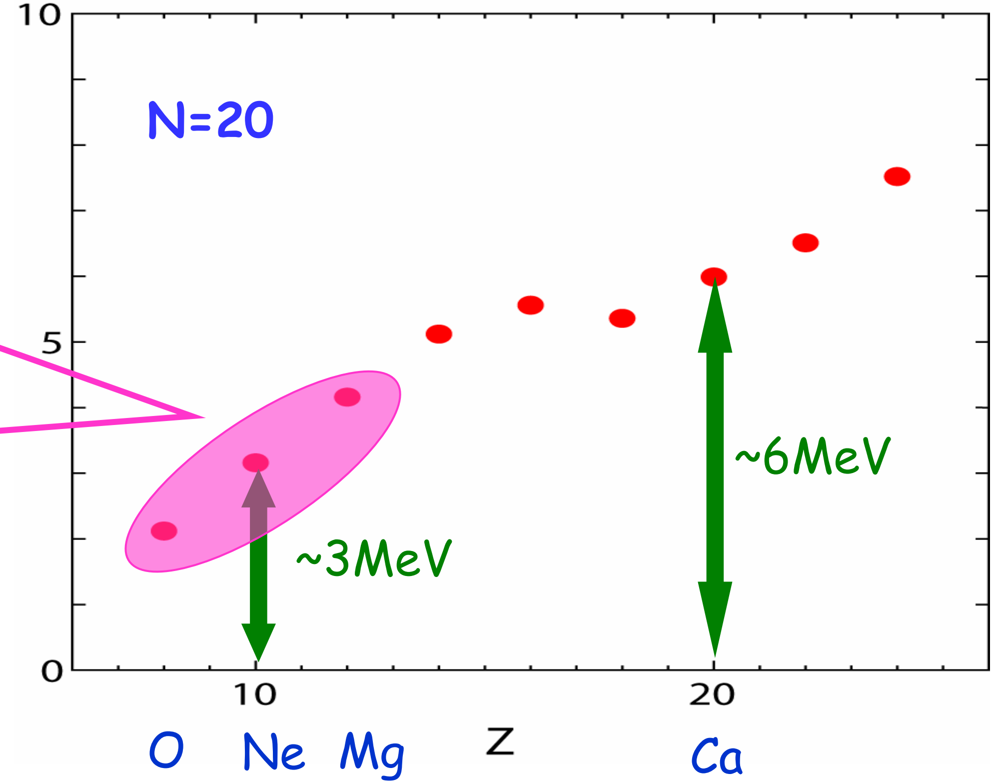

In many calculations, the gap is rather constant (5 ~ 6 MeV), and the inversion between normal and intruder ground states is basically due to different deformation energies.

Such description may not explain recent data.

The gap
(i) can be quite small,
(ii) depends on N and Z,
(iii) can vary, even if the nucleus is still far from the drip line.

What causes such changes of shell structure.

Tensor Interaction

$$V_T = (\tau_1\tau_2)\ (\ [\sigma_1\sigma_2]^{(2)}\ Y^{(2)}(\Omega)\ )\ Z(r)$$

contributes
only to **S=1** states

relative motion

π meson : primary source

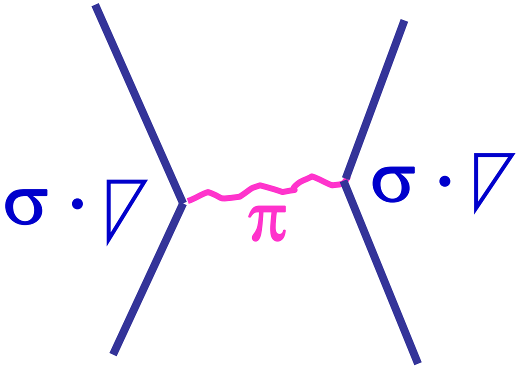

deuteron : binding, S-D coupling, Q-moment

ρ meson (~ π+π) : minor (~1/4) cancellation

Ref: Osterfeld, Rev. Mod. Phys. 64, 491 (92)

The atomic nucleus is bound due to meson exchange.
(Yukawa 1935)
Multiple pion exchanges → nuclear binding
But multiple processes are rather characterless

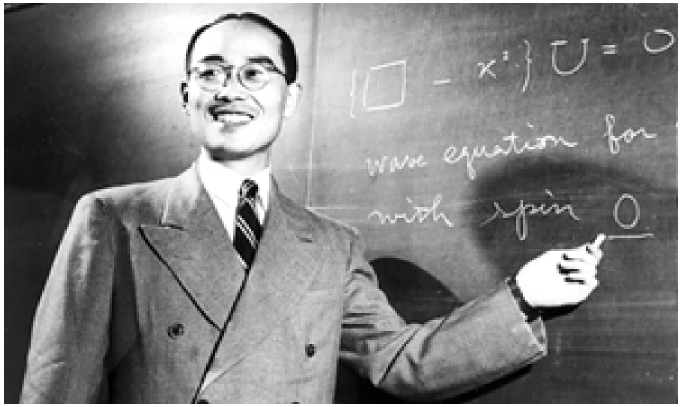

Where can we see one pion exchange ?

One pion exchange ~ Tensor force

First-order tensor force effect in spectroscopy
→ manifestation of pions in nuclei

Intuitive Picture

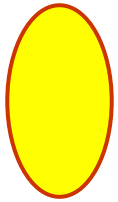

wave function of relative motion

↑↑ spin of nucleon

large relative momentum

small relative momentum

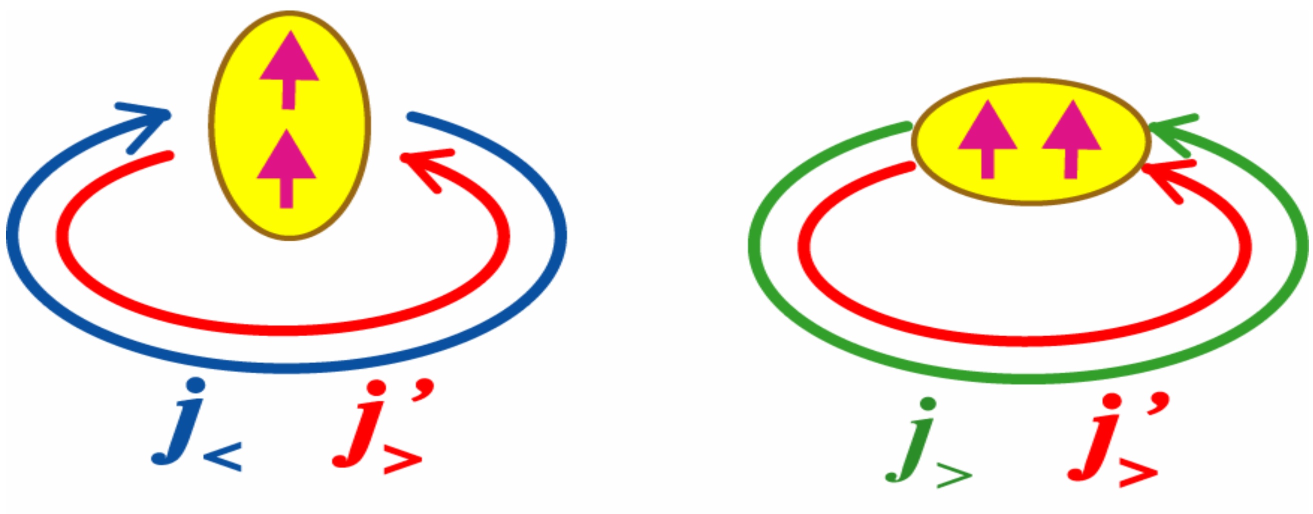

deuteron ⇨ attractive

repulsive

T. Otsuka et al., Phys. Rev. Lett. 95, 232502 (2005)

Monopole Interaction due to Tensor Interaction

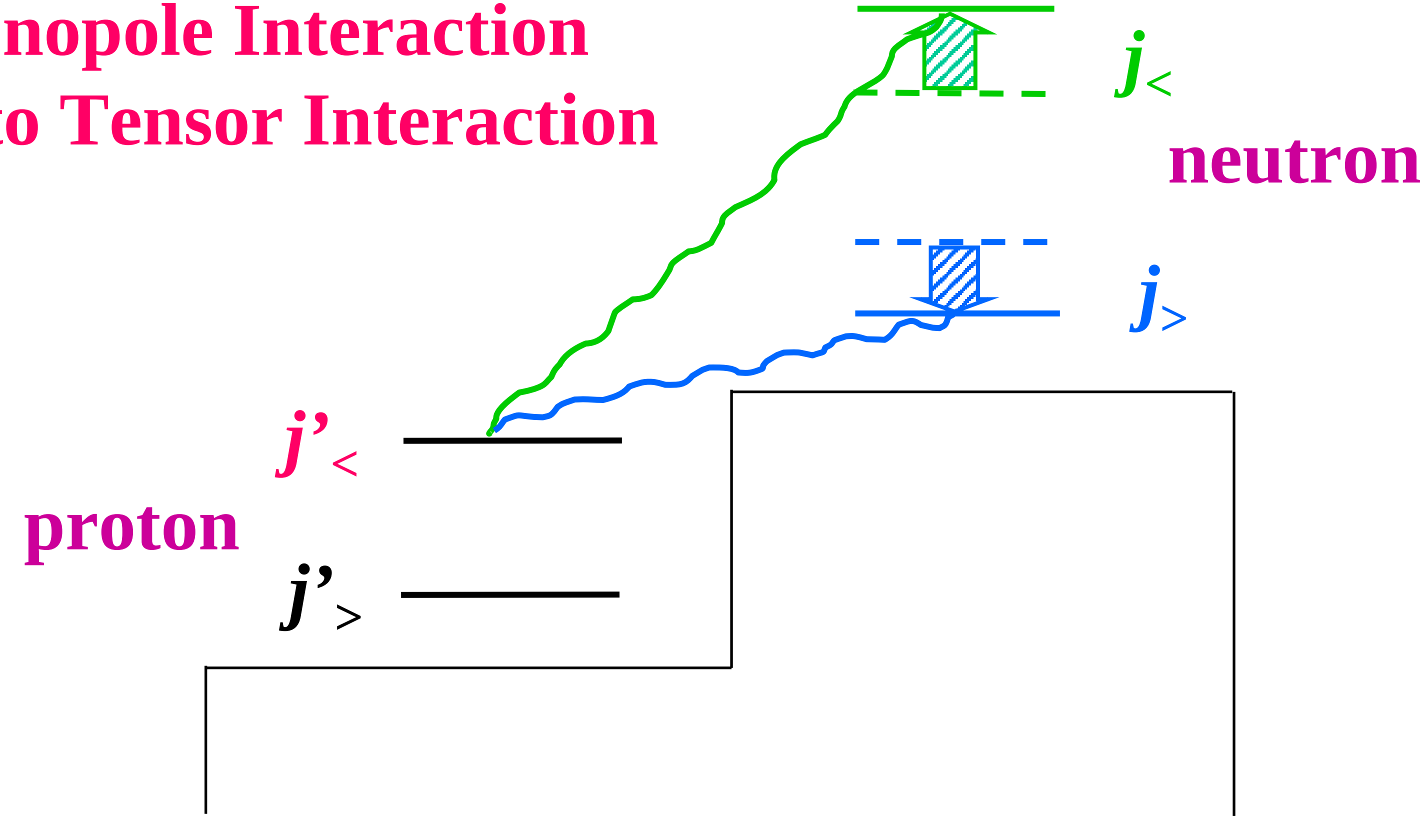

Identity for tensor monopole interaction

$$(2j_> + 1)\; v_{m,T}^{(j'\,j_>)} + (2j_< + 1)\; v_{m,T}^{(j'\,j_<)} = 0$$

$v_{m,T}$: monopole strength for isospin T

T. Otsuka et al., Phys. Rev. Lett. 95, 232502 (2005)

Tensor interaction is the primary origin of the p-n $j_>$-$j_<$ coupling.

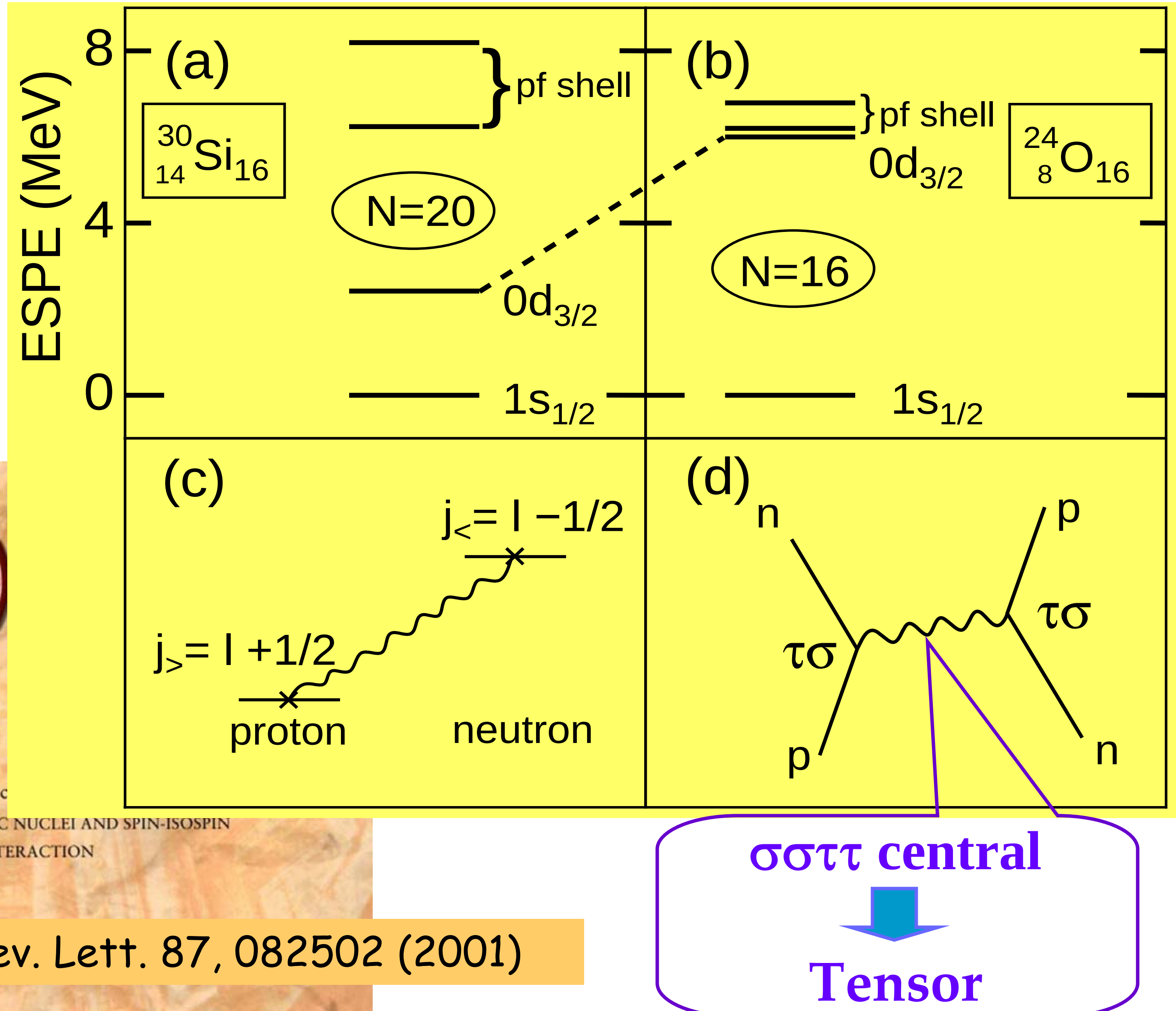

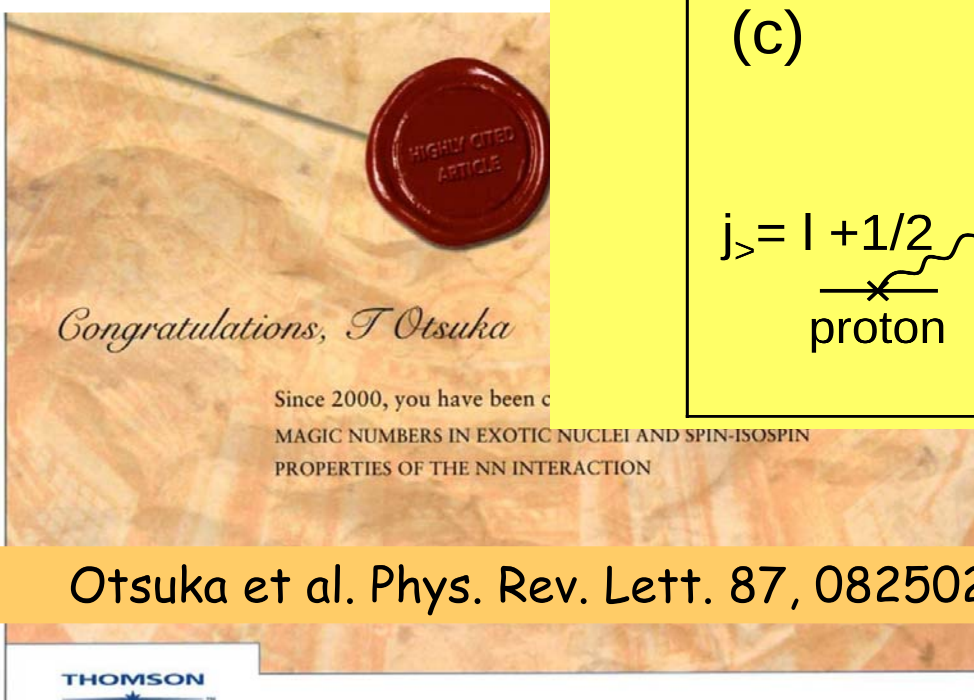

Otsuka et al. Phys. Rev. Lett. 87, 082502 (2001)

Systematic variation of neutron effective single-particle energies due to the tensor interaction ($\pi + \rho$ meson)

N=51 isotones

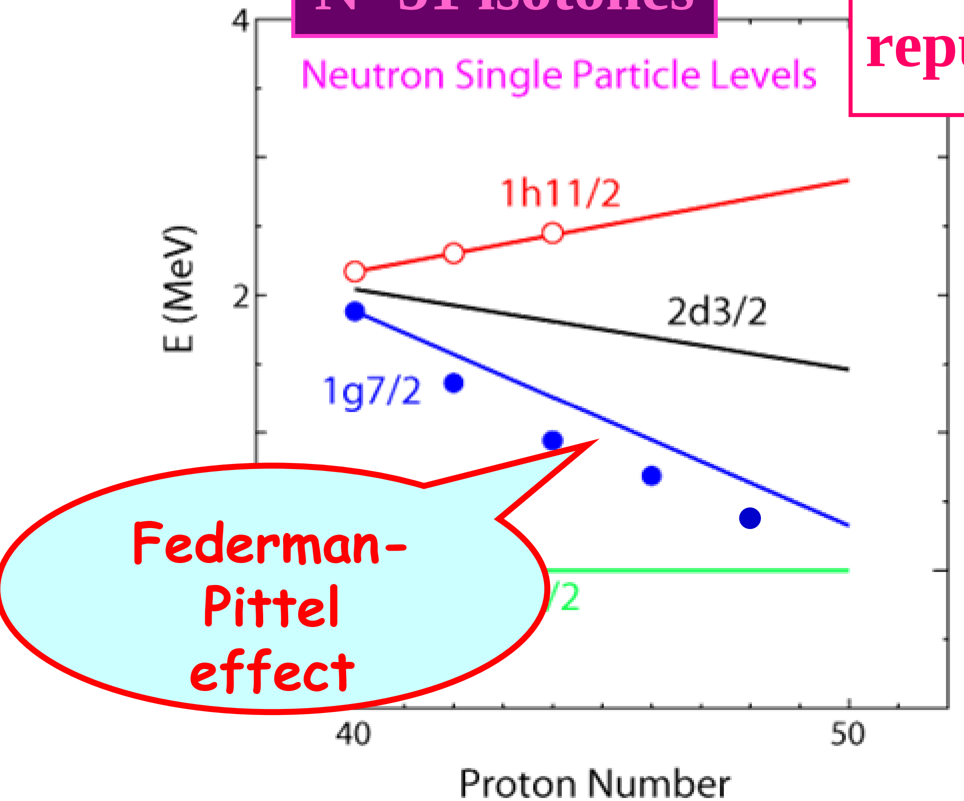

repulsion between $g_{9/2}$ and $h_{11/2}$

widening between $h_{11/2}$ and $g_{7/2}$,
not spin-orbit partner

Lines : $\pi + \rho$ meson

Points : corresponding exp. level

protons in $g_{9/2}$

Zr → Sn

shown relative to d5/2

Federman and Pittel, Phys. Lett. B 69, 385 (1977)

- Overlap of radial wave functions is emphasized -

they can simultaneously fill the $1g_{9/2}$ proton and $1g_{7/2}$ neutron orbitals. The strong overlap of these spin-orbit-partner orbitals can lead to important n-p correlations in this region and thus to deformation.

At this point it is useful to generalize our earlier remarks as to when strong n-p correlations should occur. As noted earlier, the crucial criterion is that the neutrons and protons occupy orbitals with good overlap. It was pointed out long ago [8] that the overlap between two orbitals $(n_N\, l_N\, j_N)$ and $(n_P\, l_P\, j_P)$ is maximum if $n_N = n_P$ and $l_N \approx l_P$. So far, we have focussed on cases in which $n_N = n_P$ and $l_N = l_P$, although we have emphasized that j_N need not be the same as j_P.

Summary

N=20 gap varies and can be small for Ne-Na-Mg
(independently of the distance to the drip line)

^{31}Mg, ^{29}Na, ^{30}Na and many others

"Island of Inversion" is bigger and has wide reefs

Shell evolution due to tensor interactions

-drives $j_>$ or $j_<$ levels in a specific and robust way
intuitive picture → many cases expected from p-shell to superheavies

- is the dominant origin of shell evolution

- N=20 gap also largely due to the tensor force

- **Federman-Pittel mechanism (g9/2-g7/2,h11/2)**

-Installation of tensor effect into mean field models (GT2)
→ Abe

Central forces :

Complex origins

Multiple meson exchange,
hard core (quarks, QCD may be needed)
3-body forces

Present form of Gogny interaction
good also because of full spin-isospin channels

Tensor force :

Simpler origin

dominated by one pion exchange (of course ρ, higher order ...)

Config. dependent effects → Density Functional form ... ?
Mean field formalism needed ?

←→ Chiral Perturbation

Collaborators

Y. Utsuno	JAAE	
M. Honma	U. Aizu	Shell model
T. Mizusaki	Senshu U.	
T. Suzuki	Nihon U.	
R. Fujimoto	U. Tokyo	Tensor force
H. Grawe	GSI	
Y. Akaishi	KEK	
D. Abe	Tokyo	GT2
T. Matsuo	Hitachi Ltd.	